Int. J. Electrochem. Sci., 7 **(2012)** 2596 - 2615

International Journal of
ELECTROCHEMICAL
SCIENCE
www.electrochemsci.org

Thermolysis and Conductivity Studies of Poly(Ethylene Oxide) (PEO) Based Polymer Electrolytes Doped with Carbon Nanotube

Suriani Ibrahim[*], *Mohd Rafie Johan*

Advanced Materials Research Laboratory, Department of Mechanical Engineering, University of Malaya, 50603 Kuala Lumpur, Malaysia
[*]E-mail: sue_83@um.edu.my

Received: 15 October 2011 / *Accepted:* 27 January 2012 / *Published:* 1 March 2012

In this research, solution-casting technique was employed for the preparation of solid polymer electrolytes poly(ethylene oxide) (PEO) films were characterized via differential scanning calorimetry (DSC), impedance spectroscopy (IS) and Thermogravimetric (TGA). With addition of varies of lithium hexaflurote ($LiPF_6$), ethylene carbonate (EC) and amorphous carbon nanotube (αCNT), the endothermic peak continuously decrease from 69 to 61 °C. The conductivity values for PEO complexes increased continuously and reached a maximum of 10^{-3} Scm^{-1} when 5wt% αCNTs was added into the PEO complexes. Thermogravimetric analysis (TGA) results showed that the amount of $LiPF_6$, EC and αCNT has a significant effect on the thermal stability of polymer complexes. The TGA curves also indicated that the thermal behaviour of composites polymer electrolytes differs significantly between low temperature (>100 °C) and high temperature (200 °C) range.

Keywords: polymer electrolyte; thermal stability; decomposition; thermolysis; phase transitions

1. INTRODUCTION

Polymer electrolytes have gained much interest due to their potential applications such as lithium rechargeable batteries and fuel cell [1,2]. Polymer electrolytes are flexible and possess the ability to transform into desired shapes. Moreover, the flexible polymers can accommodate the shape changes during charge-discharge cycle. The development of polymeric systems with high ionic conductivity is one of the main objectives in polymer research, due to their potential application in electronics such as solid state rechargeable lithium batteries, electrochromic windows, etc [3,4]. The discovery of ionic conductivity in polyether-based hosts complexed with alkali metal salts by Fenton et

al. [5] and Wright [6] has generated research activities leading to significant advances in the characteristics and structure of these polymer-salt complexes.

Poly(ethylene oxide) has been a popular choice of polymer matrix for lithium ion conductors [7]. $LiPF_6$ is the most common lithium salt employed in lithium-ion batteries as it offers good electrolyte conductivity and film forming. Studies have proved that in PEO based polymer electrolytes systems, conductivity will increase as the salts concentrations increases [8-12]. Solid polymeric electrolytes consist of salt dissolved in a polymer matrix forming an ion-conducting solid solution [13]. However, for this application, the polymer has to possess certain properties, such as amorphous character, oxygen molecules in its structure, low glass transition temperature, electrochemical and dimensional stability, mechanical resistance and the possibility of forming relatively thin films or pellets [13]. By investigating the thermal behaviour of polymers as a function of weight loss with heat, it is possible to obtain information about their stability.

To the best of the authors' knowledge, little attention has been paid on the compatibility and thermal stability studies of PEO polymer electrolytes. Also, the salts commonly used in lithium battery electrolytes such as $LiPF_6$, $LiAsF_6$ and $LiBF_4$ have poor thermal stability and may have toxic by-products. Hence, the objective of this research is to investigate the thermal behaviour of salted polymer. Among the salts commonly used, an attempt has been made to choose the best salt for lithium batteries in terms of thermal, electrochemical and compatibility view point. Thermogravimetric analysis (TGA) can be used as a way to measure the thermal stability of a polymer and the thermal degradation of polymer due to the simplicity of the weight loss method [14]. The neural network model has been developed and it was successful to predict the role of salt, plasticizer and filler for the ionic conductivity enhancement in the nanocomposites polymer electrolyte system [15, 16].

In this work, differential scanning calorimetry (DSC), impedance spectroscopy (IS) and Thermogravimetric analysis were used to analyze the phase transition, conductivity and thermal behavior in a series of PEO complexes. This work is aimed to examine the thermal properties associated with the conductivity of novel nanocomposite solid polymer electrolytes.

2. EXPERIMENTAL

Polymer electrolytes were prepared by standard solution-casting techniques. PEO (MW = 600,000, Acros Organics) was used as host polymer matrix, lithium hexaflurosphosphate ($LiPF_6$) (Aldrich) as the salt for complexation and ethylene carbonate (EC) (Alfa Aesar) as plasticizer. Amorphous carbon nanotube (αCNT) was prepared by chemical route at low temperature [17] . Prior to use, PEO was dried at 50 ^oC for 48 hours. Appropriate quantities of PEO, $LiPF_6$, EC and αCNT were dissolved separately in acetonitrile (Fisher) and stirred well for 24h at room temperature to form a homogeneous solution. All samples were stored under dry conditions. An electronic digital caliper was used for measuring films thickness and average thickness for films is 0.76mm. The ionic conductivities of the samples were measured at temperature ranging from 298 to 373 K using HIOKI 3531 LCR Hi-Tester with frequency range of 50 Hz to 5 MHz. Differential Scanning calorimeter (DSC) thermographs were generated using DSC 820 fitted with 56

thermocouples. Thermogravimetric analysis (TGA) data for the polymer composite were collected using TGA/SDTA 851 Mettler Toledo.

3. RESULTS & DISCUSSION

3.1. Conductivities studies

3.1.1. Various $LiPF_6$ salt concentrations

Fig. 1 shows the plot of conductivity dependence temperature at various weight percent of $LiPF_6$. The temperature dependence of the ionic conductivity is not linear and obeys the VTF (Vogel-Tamman-Fulcher) relationship. The conductivity of salted polymer electrolytes is found to increase with temperature, from 303 to 373K. At higher temperature, the thermal movement of polymer chain segments and the dissociation of salts were enhanced the ionic conductivity [18].

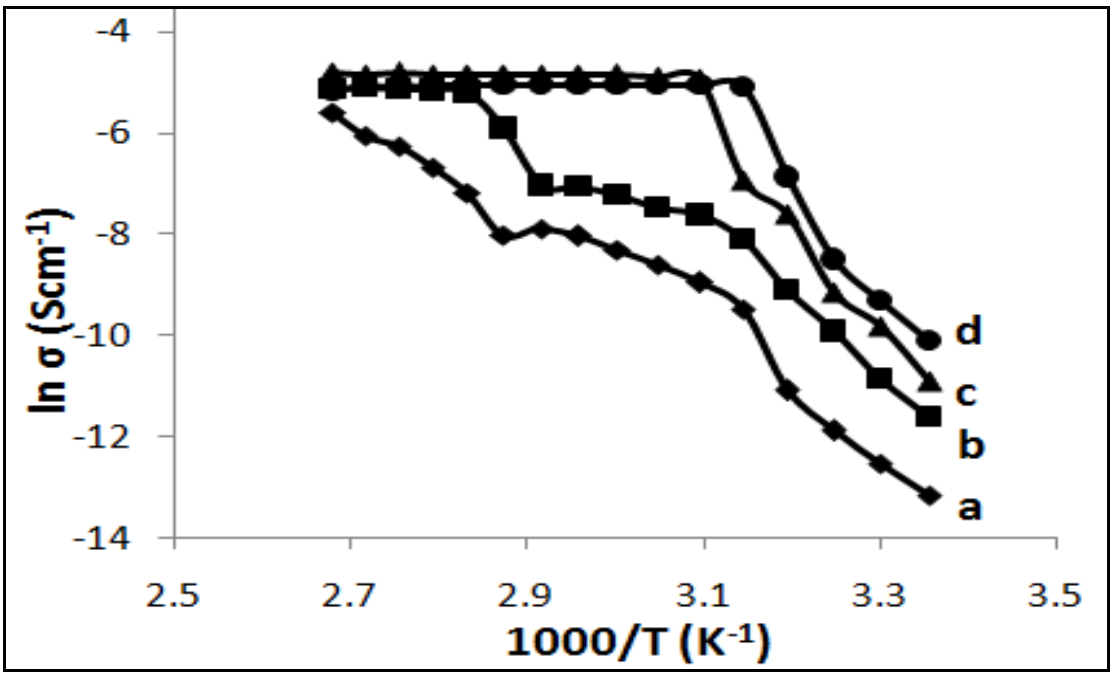

Figure 1. Conductivity dependence temperature of polymer electrolytes at various wt% of $LiPF_6$ (a) 5 ; (b) 10 ; (c) 15 ; (d) 20.

3.1.2. Various EC plasticizer concentrations

Fig. 2 shows the plot of ionic conductivity temperature dependence at various wt% of EC. The temperature dependence of the ionic conductivity is not linear and obeys the VTF relationship.

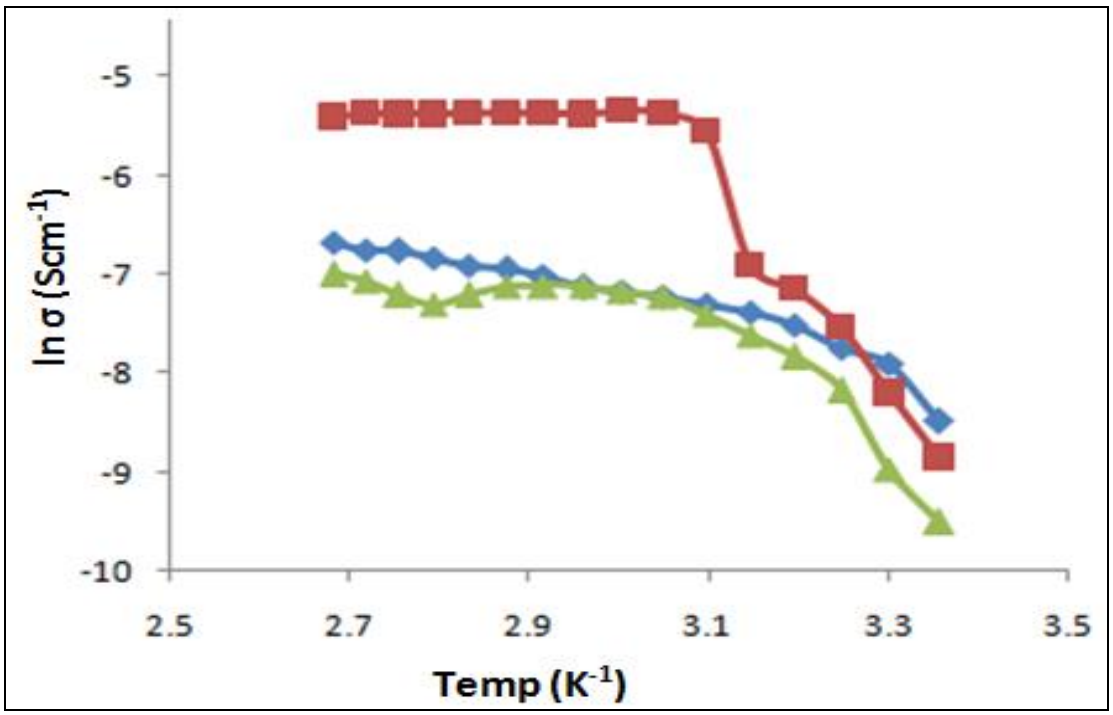

Figure 2. Conductivity dependence temperature of complexes at various wt% of EC (a) 5 ; (b) 10 ; (c) 15.

The conductivity increases with increasing temperature upon the addition of 5 and 10wt% of EC, as shown in Fig. 2. It is evident that the ionic conductivity increases with an increase in plasticizer content and temperature. This can be explained in terms of two factors, first: an increase in the degree of interconnection between the plasticizer-rich phases due to an increase in the volume fraction of these phases; and second, increase in the free volume of the plasticizer rich phase due to an increase in the relative amount of the plasticizer compared with that of PEO. At higher concentrations of plasticizer, the transport of ions may be expected to take place along the plasticizer-rich phase.

Although the improvement in conductivity in certain electrolyte systems has been interpreted in terms of plasticization of the polymer structure [19] or an alteration in the ion transport mechanism [20], other effects related to the viscosity of the ionic environment may also contribute. As the amount of plasticizer is increased, an optimum composition is reached whereby ion interactions between the solubilizing polymer and the plasticizer are such that ion mobility is maximized. A further increase in plasticizer content may eventually cause displacement of the host polymer by plasticizer molecules within the salt complexes and a decrease in ionic mobility.

3.1.3. Various CNTs filler concentrations

Fig. 3 shows the temperature dependence of conductivity for polymer electrolytes between 298 to 373K. It is evident that the room temperature conductivity increases with different wt% of αCNTs. When the organic filler was added to the polymer electrolytes, new interfaces were connected with the filler surface such as the αCNTs/polymer spherulite interfaces, which provide more effective paths for

the migration of the conductivity ions [21]. Moreover, the nanosize αCNTs improve the conduction of the mobile ions due to their extremely high surface energy [21-26]. This, prevents local PEO chain reorganization with the result of freezing at ambient temperature and a high degree of disorder, which in turn favours fast ionic transport. As the αCNTs concentration increases, the conductivity also increases due to more mobile ions which can be transported in nanocomposite polymer electrolytes. The conductivity values at room temperature for 1wt% of αCNTs is 2.2 x 10^{-4} Scm^{-1} and increases to 1.3 x 10^{-3} Scm^{-1} when 5wt% of αCNTs were added into polymer complexes. The conductivity value increases by an order of magnitude with the increase of αCNTs concentrations. However, there is a possibility of increased proton conductivity with increases αCNTs concentrations. It is well known that αCNTs are very good electronic conductors [27, 28], but the effect on proton conductivity is less studied. It is also suggested that structural modifications occuring at the αCNT surface due to the specific action of the polar surface groups of the organic filler act as Lewis acid-base interaction centers with the electrolyte ionic species [27]. Thus, it is expected that lowering ionic coupling promotes salt dissociation via a sort of ion-filler complex formation.

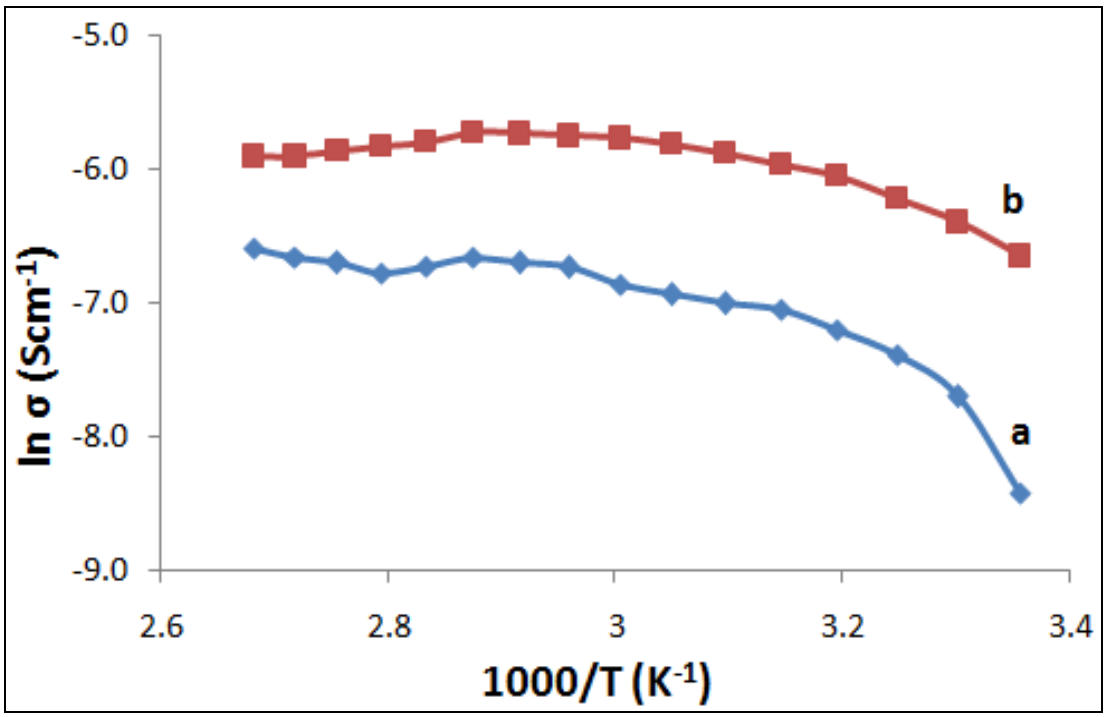

Figure 3. Temperature dependence conductivity for polymer electrolyte at different wt% of αCNTs of (a) 1 and (b) 5.

3.1.4. Optimum concentrations of nanocomposite polymer electrolytes

Fig. 4 shows the temperature dependence of conductivity for various electrolytes between 298 and 373K. It is evident that the room temperature conductivity increases with different chemical composition. The conductivity increases by 5 orders of magnitude with the addition of $LiPF_6$, 4 orders

of magnitude with the addition of EC and 3 orders of magnitude with the addition of αCNTs. The sudden increase of conductivities is due to the role of lithium ions in the PEO, the increase in flexibility of the polymer chain due to the EC and high electrical conductivity properties of αCNTs on polymer electrolytes.

There is a sudden increase in conductivity for pure PEO electrolyte at 313 – 323K (Fig. 4(a)). However, the ionic conductivity increases linearly beyond 323K. With the addition of $LiPF_6$, EC and αCNTs, the thermal effects are clearly observed in Fig. 4(b) – (d), which show a slight increase in conductivity in a wide temperature range. When EC was added into the system, more salts are dissociated into ions, which have low viscosity and therefore increases ionic mobility. The addition of αCNTs increases the conductivity by inhibiting recrystallization of the PEO chains and providing Li^+ conducting pathway at the filler surface through Lewis acid base interaction among different species in the electrolytes [29]. A transportation lithium ion within the polymer matrix requires low energy and hence increases the conductivity. This is possibly due to size of the filler and plasticizer molecule compared to the polymer molecule, which can penetrate easily into the polymer matrix [30]. The sample, which consists of $LiPF_6$, EC and αCNTs, shows lower activation energy at ambient temperature (298K ~ 373K). A transportation lithium ion within the polymer matrix requires low energy and hence increases the conductivity. This is possibly due to size of the filler and plasticizer molecule compared to the polymer molecule, which can penetrate easily into the polymer matrix [30].

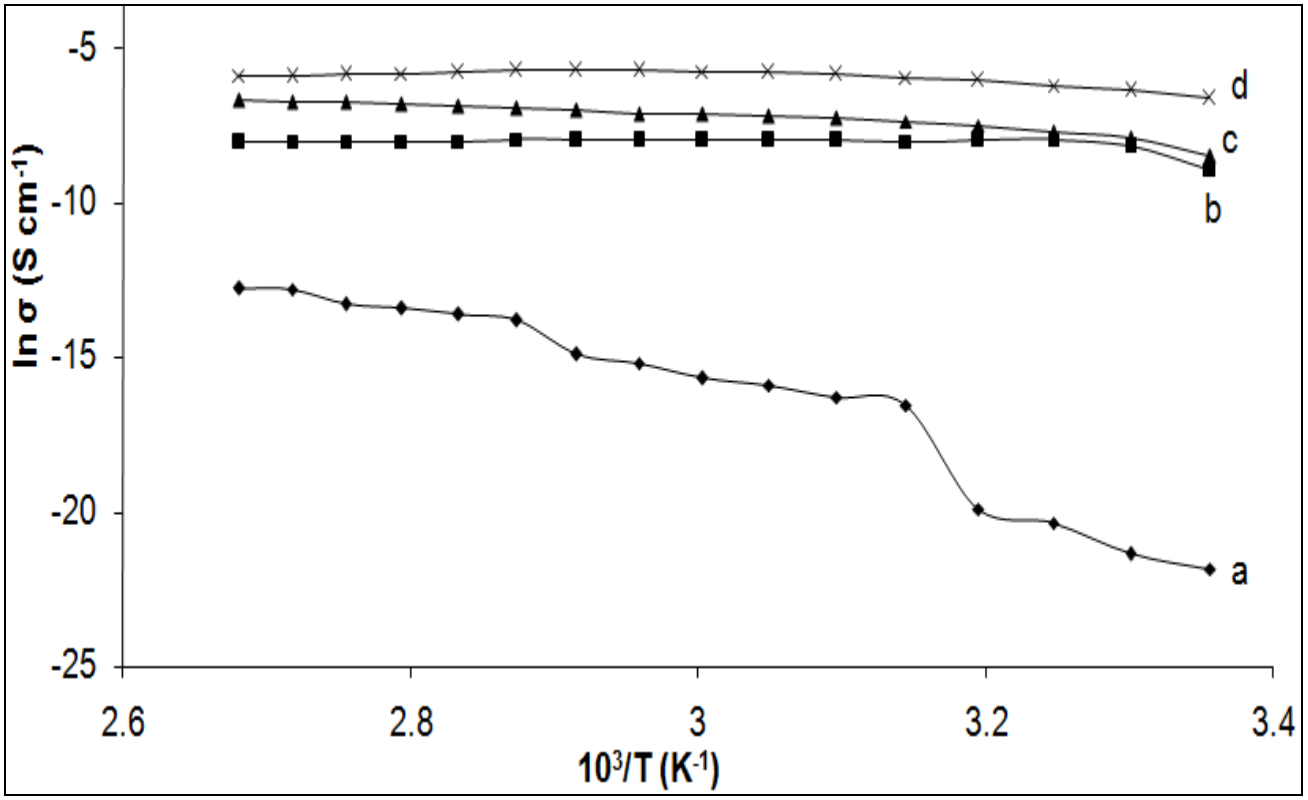

Figure 4. Conductivity dependence temperature of nanocomposite polymer electrolytes at optimum compositions (a) PEO; (b) PEO -20 wt% $LiPF_6$; (c) PEO -20 wt % $LiPF_6$ - 15 wt % EC (d) PEO -20 wt% $LiPF_6$ - 15 wt% EC -5 wt% αCNTs.

3.2 DSC studies

3.2.1 Differential scanning calorimetry (DSC) analysis of polymer electrolytes at various wt% of $LiPF_6$

Fig. 5 shows the DSC curves of polymer electrolytes at various weight percent of $LiPF_6$

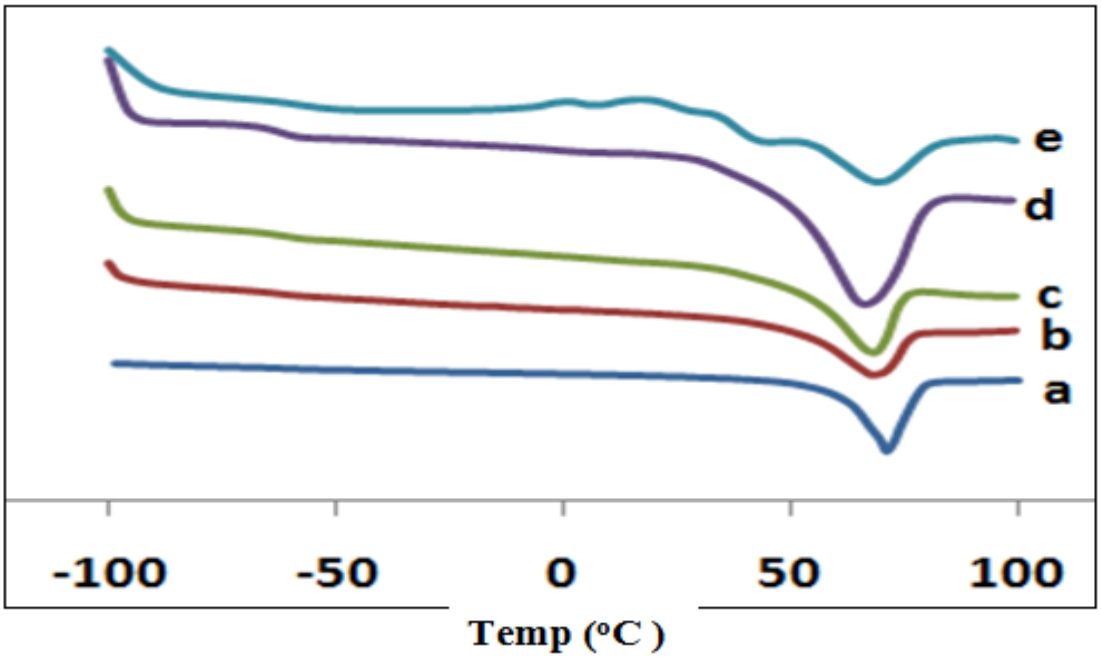

Figure 5. DSC curves of polymer electrolyte at various wt% of $LiPF_6$ (a) 0 ; (b) 5 ; (c) 10 ; (d) 15 ; (e) 20.

The sharp endothermic peak observed at 69°C corresponds to the crystalline melting temperature (T_m) of pure PEO (Fig. 5(a)). The endothermic peak for pure PEO shows a the transition from 69 to 67°C upon the addition of 5wt% of salt. The T_m value continues to decrease as more wt% of salt is added. This observation shows the reduction in T_m value by the addition of salt. The endothermic curves also indicate a reduction in PEO crystallinity. The relative percentage of crystallinity X_c of PEO has been calculated using Equation (1).

$$X_c = \frac{\Delta H_m}{\Delta H_m^o} x100\% \qquad (1)$$

where ΔH_m is the melting enthalpy estimated experimentally and ΔH_m^o used as referenced is the melting enthalpy for 100% crystalline PEO (213.7 Jg^{-1}) used as reference [31]. The calculated values of X_c are summarized in Table 1. The crystallinity degree of the electrolyte decreases with the wt% of the salt, which causes an increase in the amorphous phase. The polymeric chain in the amorphous phase is more flexible, which results in the enhancement of segmental motion of the

polymer. The reduction of T_m and X_c suggests that the interaction between the polymer host backbone and $LiPF_6$ affects the main chain dynamics of the polymer. This is due to the coordination bonds between ether units of PEO and Li^+ ions where Li^+ and PF_6^- ions interrupt the packing of PEO molecules and decrease the degree of crystallinity.

Table 1. Thermal properties of salted polymer electrolytes

Sample	T_g (^oC)	T_m (^oC)	ΔH_m(Wg^{-1})	X_c(%)
Pure PEO	-66	68.8	181.37	84.87
PEO-5wt% $LiPF_6$	-68	67.4	144.93	67.82
PEO-10wt% $LiPF_6$	-68	65.1	124.94	58.46
PEO-15wt% $LiPF_6$	-70	64.4	117.59	55.03
PEO-20wt% $LiPF_6$	-72	63.5	101.56	47.52

This will promote the amorphous phase which is expected to favour ion transport, thus enhancing the electrolytes' conductivity. The glass transition temperature (T_g) involves the freezing of large-scale molecular motion without a change in structure at which a glassy phase of the sample becomes a rubbery amorphous phase on heating. T_g of a polymer concerns with the mobility of the polymer chain. Lower T_g usually leads to easier chain relaxation, In PEO-based polymeric electrolytes, lithium ion conduction is promoted by such segmental motion in the amorphous phase. This shows that T_g is lowered when $LiPF_6$ is added which suggests that the segmental mobility of PEO in this region increases upon the addition of $LiPF_6$. An electrolyte with low T_g always implies fast ion conduction.

3.2.2. DSC Analysis of salted polymer electrolytes at various wt% of EC plasticizer

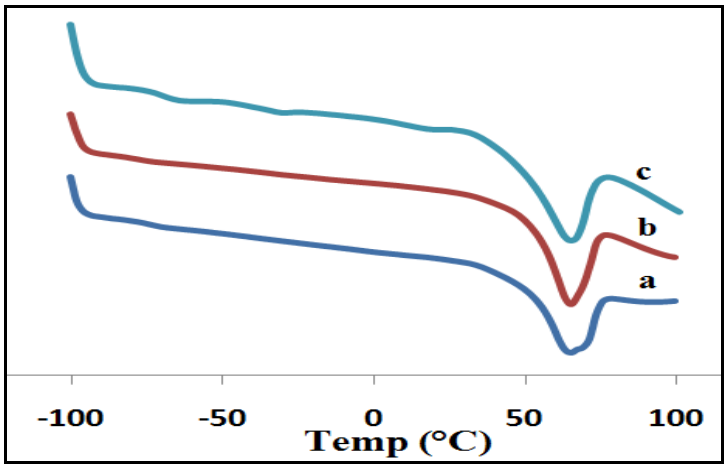

Figure 6. DSC curves of salted polymer electrolytes at various wt% of EC (a) 5 ; (b) 10 ; (c) 15

Fig. 6 shows the DSC curves of PEO:$LiPF_6$ with various wt% of EC over the temperature range of -100 to 100 ^oC. In the case of PEO-$LiPF_6$-EC mixture, the sizes of crystallinity peaks are smaller and T_m and T_g are lower than pure PEO. As the ratio of EC increases in the mixture, the relative crystallinity, X_c, T_m and T_g tend to decrease. These results seem to be caused by the addition of EC, which increases the interfacial area by phase separation, which results in the fall of crystallinity. The results obtained from the reheating cycle are summarized in Table 2. The presence of EC favours the entropy configuration of the polymer to provide more free volume, in which the ions move easily in the bulk through the plasticizer rich phase [32].

It is evident from Table 2 that there is a marked decrease in T_g, T_m and X_c during heating as a result of EC addition. The high conductivity of the samples is due to the increase of amorphous phase in the polymer with the presence of the plasticizer. It can be inferred that the amorphous phase of the polymer electrolytes facilitates fast Li-ion motion in the polymer network, which further provides a larger free volume upon temperature increase [33]. Since lithium-ion conduction in PEO-based polymer electrolytes mainly takes place in the amorphous phase, low crystallinity should be favourable for ion conduction at low temperatures.

Table 2. Thermal properties of plasticized polymer electrolytes

Sample	T_g (^oC)	T_m (^oC)	ΔH_m(Wg^{-1})	X_c(%)
PEO-20wt% $LiPF_6$-5wt% EC	-72	63.2	127.08	59.47
PEO-20wt% $LiPF_6$-10wt% EC	-74	63.1	109.55	51.27
PEO-20wt% $LiPF_6$-15wt% EC	-76	62.9	101.19	47.35

3.2.3. DSC analysis of salted plasticized polymer electrolytes at various wt.% of αCNTs filler

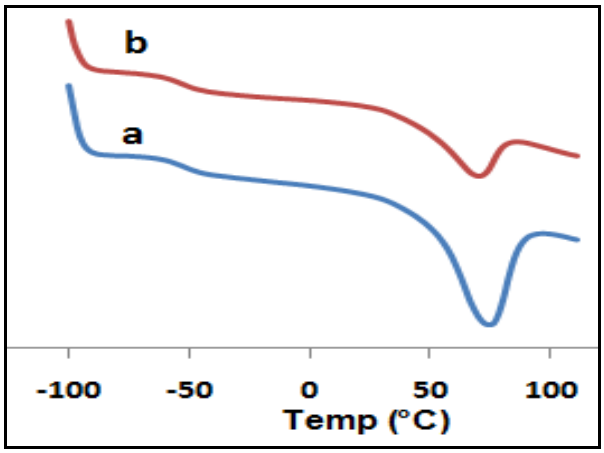

Figure 7. DSC curves of polymer electrolytes at various wt% of αCNTs (a) 1 and (b) 5.

Fig. 7 shows the DSC curves of PEO:$LiPF_6$:EC with various wt% of αCNTs over the temperature range of -100 to 100 ^oC. The results obtained are summarized in Table 3. The sharp endothermic peak corresponds to the crystalline melting temperature (T_m) and shows a slight transition from 62 to 61 °C upon the addition of 5wt% of αCNTs. The endothermic peak also indicates a reduction in PEO crystallinity. The relative percentage of crystallinity (X_c) for the electrolyte decreases with wt% of the αCNTs, which causes an increase in the amorphous phase. The polymeric chain in the amorphous phase is more flexible, which results in the enhancement of segmental motion of the polymer. The position of T_g for PEO-$LiPF_6$-EC filled with different wt% of αCNT is slightly shifted towards lower temperature. This suggests that the segmental mobility of PEO-$LiPF_6$-EC in this region increases upon the addition of αCNTs and that the segment becomes less rigid. The filler effect such as nanosized αCNTs, interacts with the PEO polymer matrix to suppress the crystallization of PEO, leading to an increase in ionic conductivity, especially at temperature lower than its melting point [34]. A similar behaviour was also observed in the PEO polymer electrolyte containing fillers such as SiO_2 and TiO_2 [34, 35]. A contribution to the conductivity enhancement comes from the structural modifications associated with the polymer host caused by the filler especially at temperatures below T_g and T_m should possibly be due to this effect. The samples clearly point towards the existence of a second conductivity enhancement mechanism, other than that involving the polymer host directly [34]. This conductivity enhancement at temperatures above as well as below T_g and T_m, should therefore be caused by a different mechanism directly associated with the surface groups in the filler [35].

Table 3. Thermal characteristics of nanocomposite polymer electrolytes

Sample	T_g (^oC)	T_m (^oC)	ΔH_m(Wg^{-1})	X_c(%)
PEO-20wt% $LiPF_6$-15wt% EC -1wt% CNT	-78	62	98.75	46.21
PEO-20wt% $LiPF_6$-15wt% EC -5wt% CNT	-80	61	57.95	27.12

3.2.4. DSC analysis of nanocomposite polymer electrolytes at optimum wt% of $LiPF_6$, EC and αCNTs

Fig. 8 shows the DSC curves for various polymer electrolytes with optimum wt% of $LiPF_6$, EC and αCNTs over the temperature range of -100 to 100^oC. The results obtained are summarized in Table 4. All polymer electrolytes exhibit endothermic peaks between 50 and 70 ^oC, which suggest the presence of a crystallization phase, based on the melting point for PEO (60 – 75 ^oC). The curves show that the addition of salt, plasticizer and filler will influence the relative degree of crystallinity (X_c), the glass transition temperature (T_g) and melting temperature (T_m) of polymer electrolytes. A sharp endothermic peak is observed near 65 ^oC during the heating process for the melting of pure PEO, as

shown in Fig. 8(a). The addition of $LiPF_6$ salt causes a change in the shape of the endothermic peak, and the peak shifts towards lower temperature.

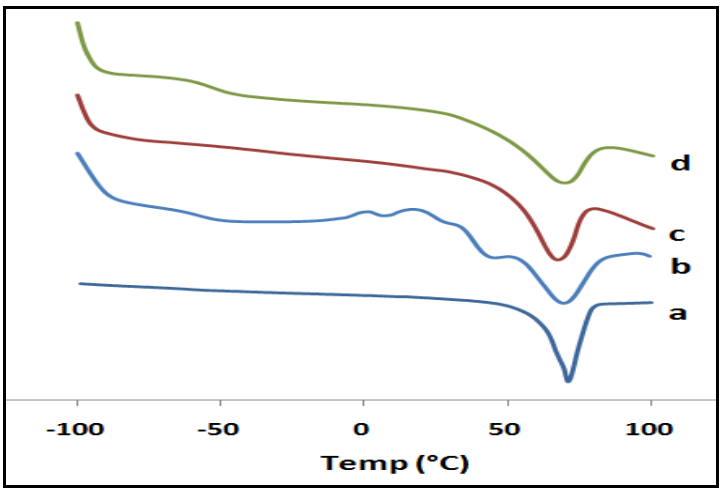

Figure 8. DSC curves of (a) PEO (b) PEO-20 wt% $LiPF_6$ (c) PEO-20 wt% $LiPF_6$-15 wt% EC (d) PEO-20 wt% $LiPF_6$-15 wt% EC-5 wt% αCNTs.

This also indicates the complexation process between $LiPF_6$ and PEO. The T_g and T_m continues to decrease with the addition of plasticizer (EC). The addition of filler (αCNTs) causes peak broadening.

Table 4. Thermal characteristics of nanocomposite polymer electrolytes

Sample	T_g (^oC)	T_m (^oC)	ΔH_m(Wg^{-1})	X_c(%)
Pure PEO	-66	68.8	181.37	84.87
PEO-20wt% $LiPF_6$	-72	63.5	101.56	47.52
PEO-20wt% $LiPF_6$-15wt% EC	-76	62.9	101.19	47.35
PEO-20wt% $LiPF_6$-15wt% EC -5wt% CNT	-80	61.0	57.95	27.12

The peak slightly shifted toward lower temperature. These observations clearly suggest that a major contribution of conductivity enhancement comes from structural modifications associated with the polymer host caused by the salt, plasticizer and filler [36]. The reorganization of polymer chain may be hindered by the cross-linking centres formed by the interaction of Lewis acid groups of filler

with the polar groups of polymer [37]. Consequently, the degree of crystallization of the polymer matrix decreases with the addition of filler [37].

It is evident that there is a marked decrease in T_g, T_m and X_c during heating upon the addition of salt, plasticizer and filler. Therefore, a significant contribution to the observed conductivity enhancement in the salt, plasticized and filler-added electrolyte, PEO + 20 wt% $LiPF_6$+15 wt% EC+5 wt% αCNTs, having the lowest T_g and T_m values, evidently comes from the increased segmental flexibility and the increased amorphous nature of the host polymer caused by the salt, plasticizer and the filler [36]. Since lithium-ion conduction in PEO-based polymer electrolytes mainly takes place in amorphous phase, low crystallinity should be favourable for ion conduction at low temperatures.

3.3. TGA studies

3.3.1. Thermogravimetric (TGA) analysis of polymer electrolytes of various wt% of $LiPF_6$ Salt

Fig. 9 shows the TGA and DTG curves of the polymer electrolytes with various wt% of $LiPF_6$.

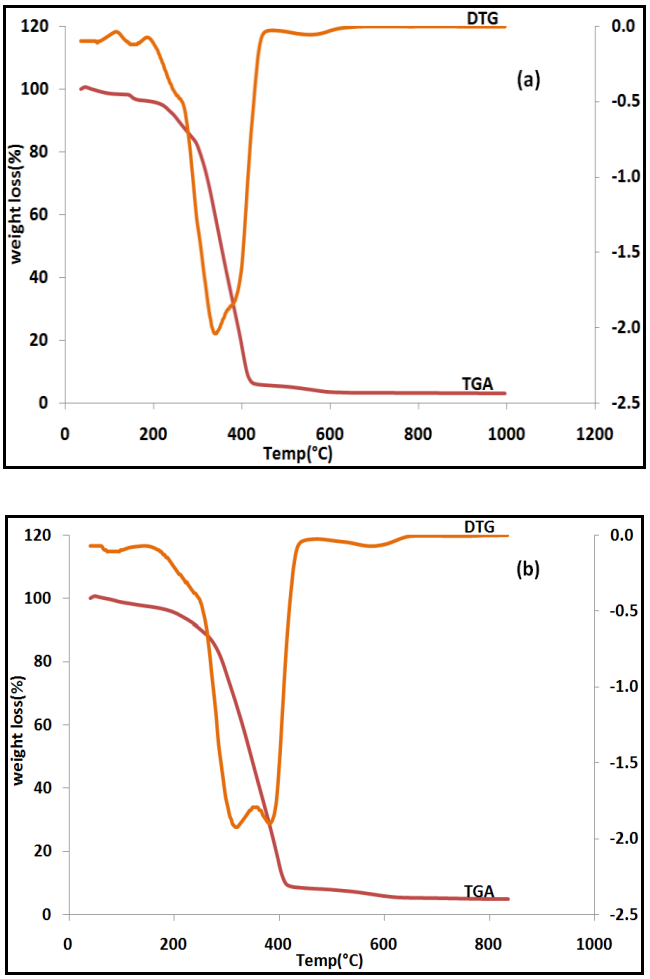

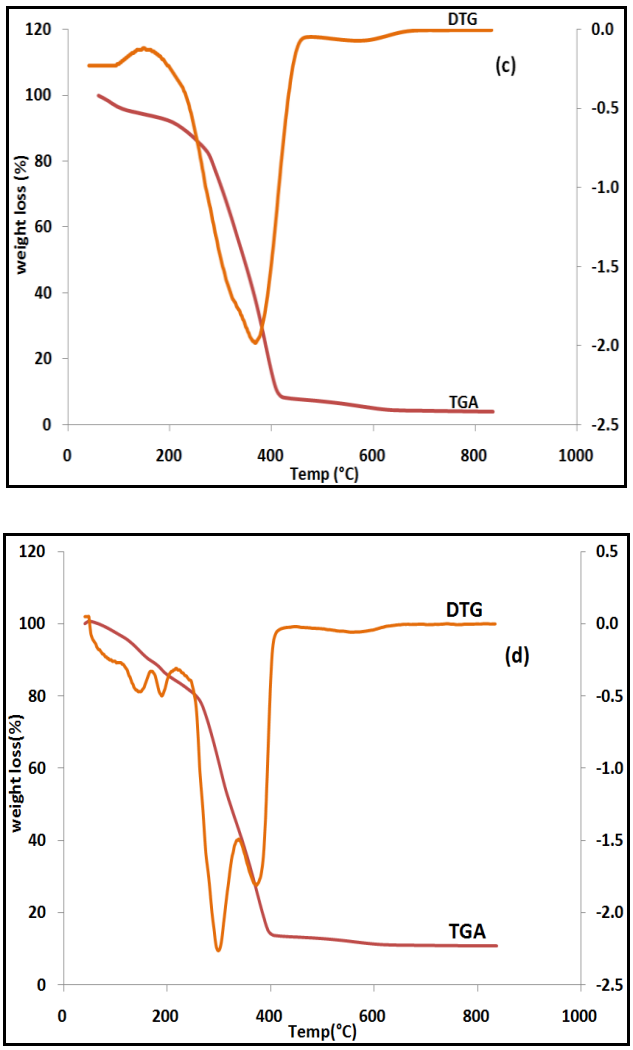

Figure 9. TG-DTG curves of polymer electrolytes at various wt% of $LiPF_6$ (a) 5; (b) 10; (c) 15; (d) 20.

Table 5. Initial and decomposition temperatures and percentage of total weight loss for various PEO-$LiPF_6$ samples

Sample	Initial Weight Loss Temperature	Weight Loss	Decomposition Temperature	Weight Loss	Total Weight Loss
	(°C)	(%)	(°C)	(%)	(%)
PEO+5wt% salt	48	8	230	88.45	96.45
PEO+10wt% salt	70	9	250	84.84	93.84
PEO+15wt% salt	80	8	230	87.00	95.00
PEO+20wt% salt	85	20	280	68.00	88.00

The TGA and DTG curves of the PEO-salt films reveal two main weight loss regions, which appear as two peaks in the DTG curves. The first region at a temperature of 40-100°C is due to the evaporation of physically weak and chemically strong H_2O bonding. The second transition region of around 230-280°C is due to decomposition of PEO-salt membrane. It can be clearly seen that all samples exhibit minimal weight loss until the samples reached 200 ºC, at which an endothermic peak appears. This indicates that the PEO-$LiPF_6$ is stable up to 200 ºC before decomposition. At 200°C, the $LiPF_6$ starts to melt and the system is no longer stable. The results of weight-loss ratios for all samples accelerating between 200 and 400 °C are summarized in Table 5.

3.3.2. Thermogravimetric (TGA) analysis of salted polymer electrolytes at various wt% EC plasticizer

Fig. 10 shows the TGA and DTG curves of the polymer electrolytes with different wt% of EC.

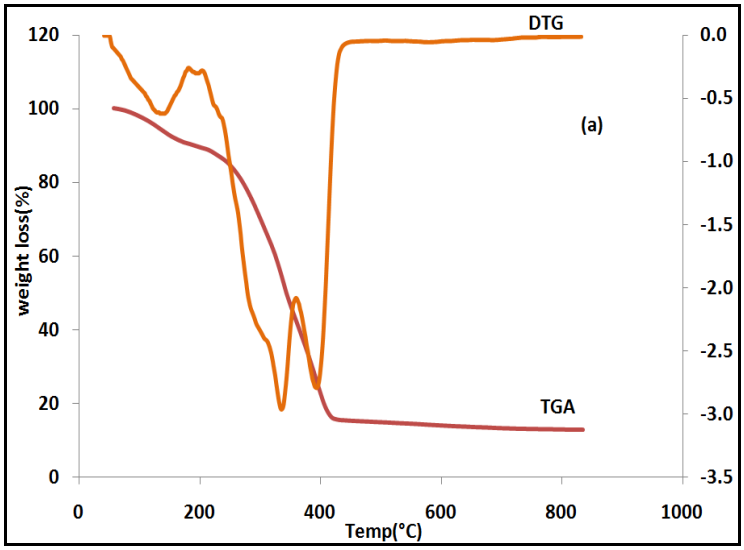

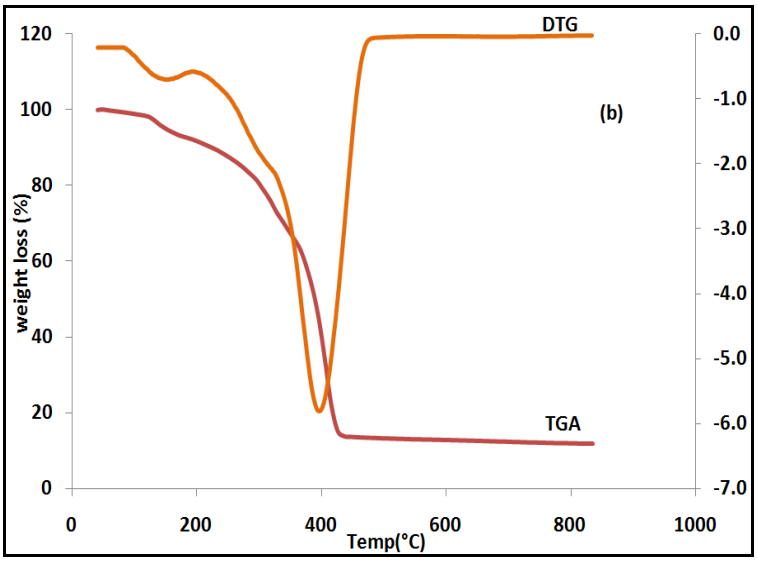

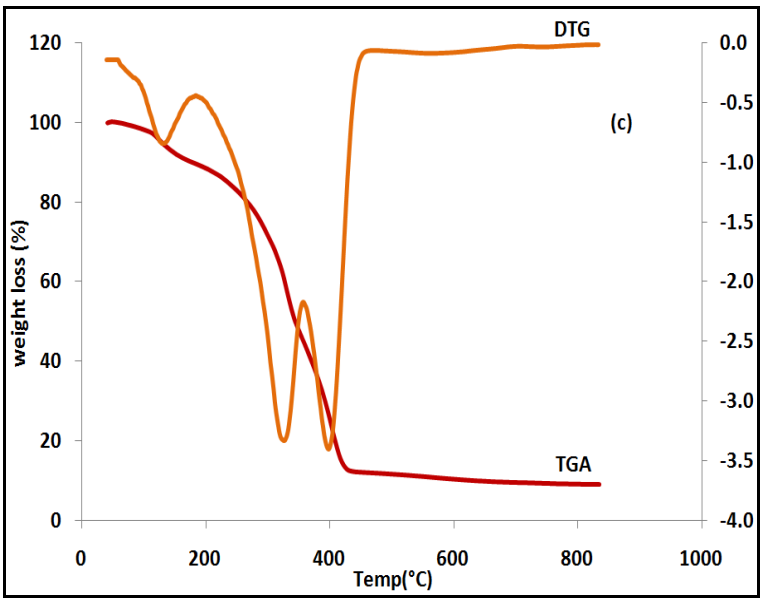

Figure 10. TG-DTG curves of salted polymer electrolytes at various wt% of EC (a) 5; (b) 10; (c) 15.

The DTG curves display two main inflection regions. The first region at lower temperatures (<100°C) originates from the loss of absorption water and solvent whereas the region at higher temperature (200°C) is associated with the decomposition of PEO.

As seen from DTG curves, the maximum temperatures of weight loss (T_m) of polymer electrolytes are 355, 396 and 376°C, respectively. It can be clearly seen that all samples exhibit minimal weight loss until the samples reached 100 ºC, at which an endothermic peak appears. The results of weight-loss ratios for all samples accelerating between 100 and 400 ^{o}C are summarized in Table 6.

From the table, it can be stated that an increase in the amount of plasticized content in the samples promotes a slight increase in weight loss.

Table 6. Initial and decomposition temperatures and percentage of total weight loss for various PEO-$LiPF_6$-EC samples

Sample	Initial Weight Loss Temperature (°C)	Weight Loss (%)	Decomposition Temperature (°C)	Weight Loss (%)	Total Weight Loss (%)
PEO+20wt% salt+5w% EC	82	8	200	80.46	88.46
PEO+20wt% salt+10wt% EC	90	10	205	80.00	90.00
PEO+20wt% salt+15wt% EC	91	9	210	81.00	90.00

3.3.3. Thermogravimetric (TGA) Analysis of Salted Plasticized Polymer Electrolytes at various wt% of αCNTs Filler

Fig. 11 shows the TGA and DTG curves of polymer electrolytes with different wt% of αCNTs.

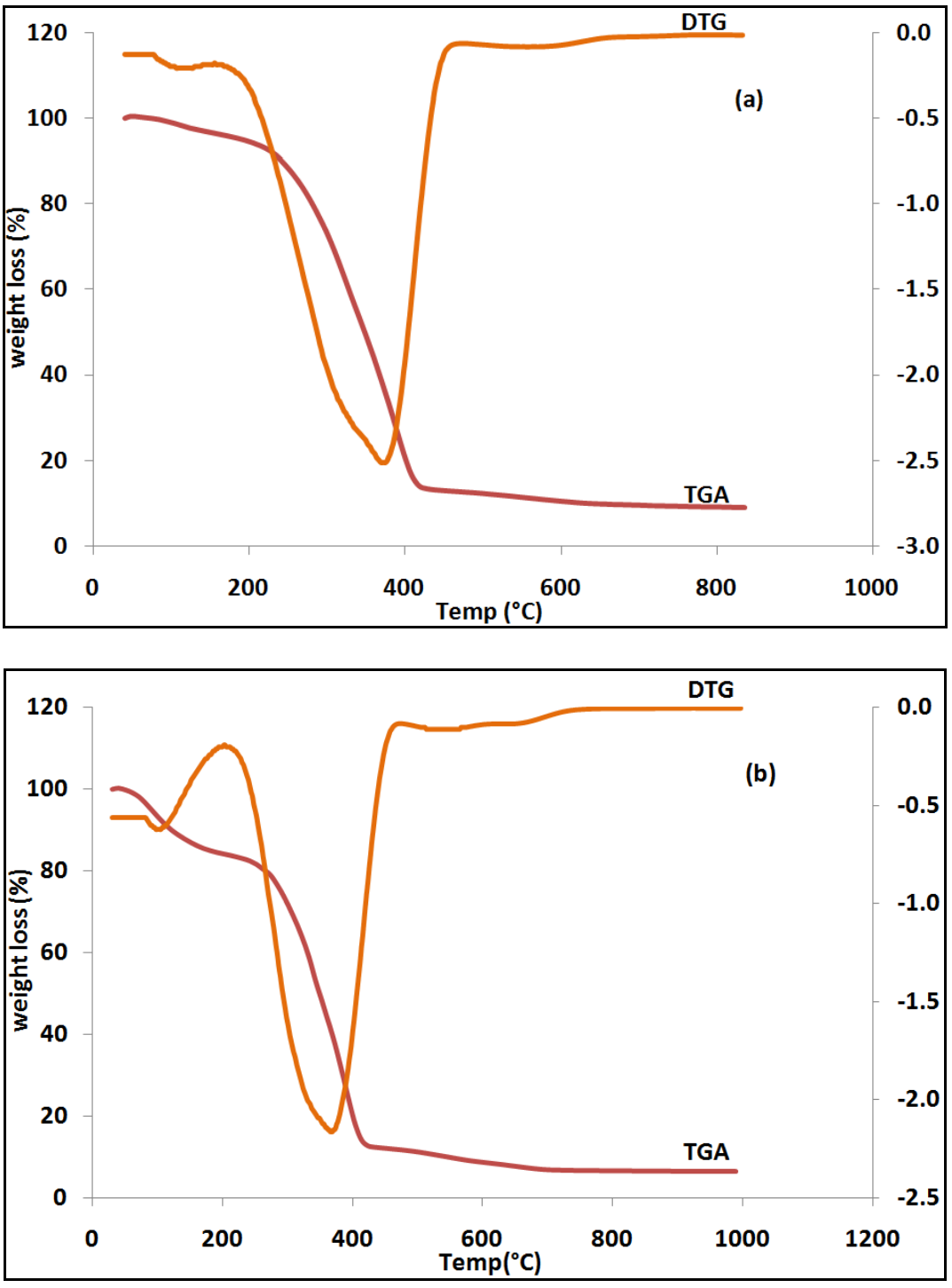

Figure 11. TG-DTG curves of polymer electrolytes at various wt% αCNTs (a) 1; (b) 5.

The results of weight-loss ratios for all samples accelerating between 100 and 400 ^{o}C are summarized in Table 7. It can be seen from Fig. 11 that the percentage weight loss for 1wt.% αCNTs is 90% and increases to 93% when 5wt% αCNTs is added into the PEO system. As the doping of αCNT nanoparticle increases, the total weight loss ratio increases, which proves that αCNT nanoparticles reduce the thermal stability of nanocomposite polymer electrolytes. Nevertheless, after subtraction of the filler mass, the thermal degradation behaviour of polymer electrolytes is only slightly affected by the αCNT content.

Table 7. Initial decomposition temperatures and percentage of total weight loss for various nanocomposite polymer electrolytes

Sample	Initial Weight Loss Temperature (°C)	Weight Loss (%)	Decomposition Temperature (°C)	Weight Loss (%)	Total Weight Loss (%)
PEO+20wt% salt+15wt% EC+1wt% CNT	97	5.2	198	84.88	90
PEO+20wt% salt+15wt% EC+5wt% CNT	198	17.0	210	76.00	93

3.3.4. Thermogravimetric (TGA) analysis of nanocomposite polymer electrolytes at optimum wt% of $LiPF_6$, EC and αCNTs

Fig. 12 shows the TGA and DTG curves weight loss of composites polymer electrolytes.

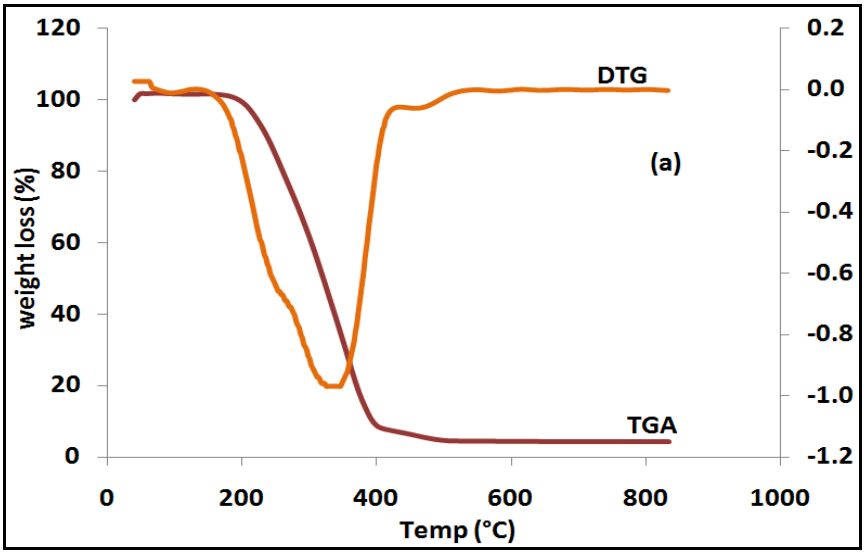

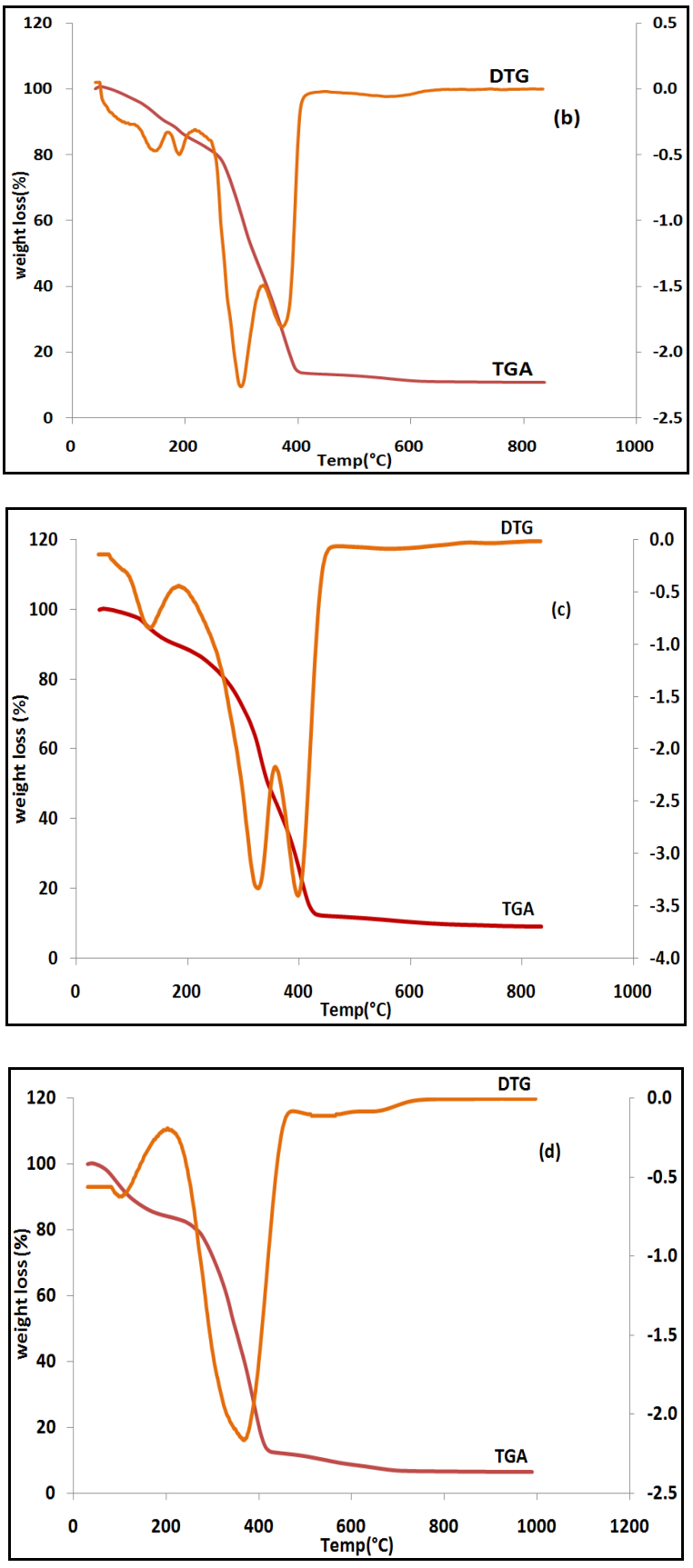

Figure 12. TG-DTG curves of nanocomposite polymer electrolytes (a) PEO; (b) PEO+$LiPF_6$; (c) PEO+$LiPF_6$+EC; (d) PEO+$LiPF_6$+EC+αCNTs

The sample shows the lost weight at around 25-100°C, which is complete at around 200-280°C. This decomposition temperature is considerably higher than those of the liquid electrolytes currently used in lithium batteries [38]. The weight loss process of the solid polymer electrolytes is gradual rather abrupt, as in the case for liquid electrolytes. For this reason, solid polymer electrolytes are more thermally stable than liquid electrolytes for applications in lithium ion batteries. Table 8 summarizes the results for optimum concentrations of solid polymer electrolytes.

Table 8. First and second decomposition temperatures and percentage of total weight loss for various nanocomposites polymer electrolytes

Sample	Initial Weight Loss	Weight Loss	Intermediate Weight Loss	Weight Loss	Total Weight
	Temperature (°C)	(%)	Temperature (°C)	(%)	Loss (%)
PEO	75	0.22	200	88.74	88.96
PEO+20wt% salt	85	20	280	68.00	88.00
PEO+20wt% salt+15wt% EC	91	10	210	81.00	90.00
PEO+20wt% salt+ 15wt% EC+ 5wt% CNT	100	10.83	220	76.00	86.53

4. CONCLUSION

Novel composite solid polymer electrolytes were synthesized sucessfully via solution-casting technique. DSC thermographs exhibit a decrease in T_m, T_g and X_c values, which leads to increased conductivity for composite polymer electrolytes at 298K. It is found that the amount of $LiPF_6$, EC and CNTs could affect significantly the thermal stabilities of polymer. The addition of $LiPF_6$, EC and CNTs could reduce the thermal stability of polymer-lithium composites in the lower temperature region (>100 °C). Moreover, the multistage decomposition profile of DTG has been observed.

ACKNOWLEDGEMENTS
The authors are grateful to the support from University of Malaya under UMRG Grant (NO. RG038/09AET). Suriani Ibrahim would like to acknowledge the financial support provided by University of Malaya's tutorship scheme and PPP Grant No PS083/2009B.

References

1. B. Scrosati. Application of Electroactive Polymers, Chapman and Hall, London, 1993
2. F.M. Gray. Polymer Electrolytes, The Royal Society of Chemistry, HN, Letchworth, 1997.
3. B. Scrosati. Applications of Electroactive Polymers (Chapman and Hall, London, 1993).
4. F.M. Gray. in: Solid Polymer Electrolytes; Fundamentals and Technological Applications (VCH Publishers, New York, NY, 1991) p. 35.

5. B.E. Fenton, J.M. Parker, P.V. Wright. *Polymer* 14 (1973) 589.
6. P.V. Wright, Br. *Polymer* 7 (1975) 319.
7. G.B. Appetecchi, M. Montanino, A. Balducci, F.L. Simon, M. Winterb, S. Passerini. *J. Power Sources* 192 (2009) 599
8. M.R. Johan, S.H. Oon, S. Ibrahim, S.M.M Yassin, Y.H. Tay. *Solid State Ionics* 196 (2011) 41
9. S. Ibrahim, S.M.M Yassin, R. Ahmad, M.R. Johan. *Ionics.* 17 (2011) 399
10. T.S. Min, M.R. Johan. *Ionics*. 17 (2011) 485
11. M.R. Johan, L.B. Fen. *Ionics*. 16 (2010) 335
12. M.R. Johan, S.A. Jimson, N. Ghazali, N.A.M. Zahari, N.F. Redha. *Inter. Nat. Mater. Reas*. 102 (2011) 4
13. G. O. Machado, R. E. Prud'homme, A. Pawlicka. e-*Polymers* 3 (2007) 115.
14. Y. S. Lee, W.K. Lee, S.G. Cho, II Kim, C.S. Ha. *J. Anal. Appl. Pyrolysis* 78 (2007) 85
15. M.R. Johan, S. Ibrahim. Communications in Nonlinear Science and Numerical Simulation 17 (2012) 329
16. M.R. Johan, S. Ibrahim. *Ionics.* DOI.1007/s11981-011-0549-z.
17. M.N. Ng, M.R. Johan, *Extended abstracts,* IEEE *International NanoElectornics Conference* 2010 (INEC 2010). Vols 1 & 2. pg 392.
18. S. Rajendran, P. Sivakumar, R.B. Shanker. *Journal of Power Sources*. 164 (2007) 815
19. G.G. Cameron, M.D. Ingram, K. Sarmouk. *Polymer*. 26 (1990) 1097
20. F. Croce, S.D. Brown, S. Greenbaum, S.M. Slane, M. Salomon. *Chemistry. Materials*. 5 (1993) 1268
21. J. Przluski, M. Siekierski, W. Wieczorek. *Electrochimica Acta*. 40 (1995) 2101
22. F. Capuano, F. Croce, B. Scrosati. *Journal of Electrochemical Society*. 138 (1991) 1918
23. M.C. Borghini, M. Mastrogostino, S. Passerini, B. Scrosati. *Journal of Electrochemical Society*. 142 (1995) 2118
24. Z.Y. Wen, T. Itoh, N. Hirata, M. Ikeda, M. Kubo, O. Yamamoto. *Journal of Power Sources*. 90 (2000) 20
25. Y.W. Kim, W. Lee, B.K. Choi. *Electrochimica Acta*. 45 (2000) 1473
26. B. Kumar, L.G. Scanlon. *Solid State Ionics*. 124 (1999) 239
27. M.P. Anantram, F. Leonard. *Reports on Progress in Physics*. 69 (2006) 507
28. B.E. Kilbride, J.N. Coleman, J. Fraysse, P. Fournet, M. Cadek, A. Drury. *Journal of Applied Physics.* 92 (2002) 4024
29. J. Ulanski, P. Polanowski, A. Traiez, M. Hofmann, E. Dormann, E. Laukhina. *Synthetic Metals*. 94 (1998) 23
30. D.K. Pradhan, B.K. Samantaray, R.N.P. Choudhary, A.K. Thakur. *Ionic*s. 11 (2005) 95
31. A.M.M.A. Ali, R.H.Y. Subban, H. Bahron, T. Winnie, F. Latif, M.Z.A. Yahya. *Ionics*, 14 (2008) 491
32. S.A. Agnihotry, S.S. Pradeep, Sekhon. *Electrochimica Acta* 44 (1999) 3121
33. M.Z.A. Yahya, A.K. Arof A.K. *European. Polymer Journal.* 38 (2002) 1191
34. G.B. Appeteechi, F. Crose , L. Persi, F. Ronci, B. Scrosati. *Electrochimica Acta* 45 (2001) 1481
35. S.H. Liao, C.Y. Yena, C.C. Wenga, Y.F. Lina, C.C. Maa, C.H. Yang, M.C. Tsai, M.Y. Yena, M. C. Hsiao, S.J. Leed, X. F. Xiee, Y. H. Hsiao. *Journal of Power Sources*. 185 (2008) 1225
36. Taner Ozel, Anshu Gaur, J. A. Rogers, Moonsub Shim. *Nano Letters*. 5 (2005) 905
37. A. Change, M. Carreb, P. Willmann. *Journal of Power Sources*. 109 (2002) 203
38. Y. Kong,, J.N. Hay. *Polymer*. 43 (2002) 3873